Compact temperature-insensitive modulator based on a silicon microring assistant Mach–Zehnder interferometer*

Zhang Xue-Jian(张雪键), Feng Xue(冯 雪)†,
Zhang Deng-Ke(张登科), and Huang Yi-Dong(黄翊东)

State Key Laboratory of Integrated Optoelectronics, Department of Electronic Engineering, Tsinghua University, Beijing 100084, *China*

(Received 6 April 2012; revised manuscript received 9 May 2012)

On the silicon-on-insulator platform, an ultra compact temperature-insensitive modulator based on a cascaded microring assistant Mach–Zehnder interferometer is proposed and demonstrated with numerical simulation. According to the calculated results, the tolerated variation of ambient temperature can be as high as 134 °C while the footprint of such a silicon modulator is only 340 μm^2.

Keywords: integrated modulator, temperature sensitivity, microring, Mach–Zehnder interferometer

PACS: 42.60.Da, 42.60.Fc, 42.79.Hp, 42.82.Ds **DOI:** 10.1088/1674-1056/21/12/124203

1. Introduction

Silicon photonics has been attracting more and more attention in recent years due to its compatibility with standard CMOS processes, which has great potential for application in intra/inter chip optical interconnection. The electro-optic modulator, in which an optical carrier wave can be modulated by a high speed electronic data signal, is one of the fundamental components in optical transmission links. The silicon modulator is competitive compared with different types of modulators because of its CMOS compatibility. Modulation in silicon can be classified as electro-refractive or electro-absorptive. Since the Pockel effect, which causes electro-absorption, is very weak in pure silicon at a telecommunication wavelength of 1.55 μm, most silicon modulators are based on electro-refractive modulation due to the plasma dispersion effect.[1] Generally, the modulation speed and depth, optical bandwidth, insertion loss, footprint, temperature stability, and power consumption are the main figures of merit of a modulator. There are two common structures for Si electro-refractive modulators: the Mach–Zehnder interferometer (MZI) and the resonant cavity. For an MZI modulator, the temperature stability is very high but it suffers from a large footprint and high power consumption. For example, the length of the most compact MZI modulators reported up to now is longer than 200 μm with a drive voltage of 1.8 V.[2] So, such a type of modulator is hard to use in chip-scale integration. On the contrary, the footprint of those based on a resonant cavity can be very small since high-Q resonance is utilized to obtain a deep modulation depth and reduce power consumption. However, due to the large thermo-optic coefficient of silicon ($\sim 1.86 \times 10^{-4}$ K^{-1}), resonant electro–optic modulators suffer from high temperature sensitivity.[1] Several approaches have been proposed and demonstrated to deal with such problems. One of the approaches is to adopt a polymer coating with a negative thermo–optic coefficient.[3] This method is effective but not compatible with standard CMOS processes. Another approach is to use an active compensation scheme,[4] in which the extra power consumption is considerable. Guha *et al.*[5] proposed and demonstrated a new structure based on a ring resonator coupled to an MZI, where the waveguide width of one arm of the MZI is carefully designed to reduce the spectrum drift in a temperature span of 80 °C. However, the arm length of the MZI is still very long

*Project supported by the National Basic Research Program of China (Grant Nos. 2011CBA00608, 2011CBA00303, 2011CB301803, and 2010CB327405), the National Natural Science Foundation of China (Grant Nos. 61036011 and 61036010), and the Project of Science and Technology from the Communication Information Security Control Laboratory.

†Corresponding author. E-mail: x-feng@tsinghua.edu.cn

© 2012 Chinese Physical Society and IOP Publishing Ltd

(∼800 μm). Recently, Green *et al.*[2] demonstrated a new approach combining the MZI and photonic crystal waveguide together to realize Si modulator with both high temperature stability (large optical bandwidth) and small footprint. The length of the phase shifter in an MZI modulator is reduced by the slow-light effect of a photonic crystal waveguide, since an larger group index ($n_{\rm g}$) can introduce larger phase-shift for a given refractive index change of material. The photonic crystal waveguide is used in the slow-light region and $V\pi L < 0.056$ V·cm is achieved. But this approach suffers from the complex fabrication process of photonic crystal structure.

In this paper, we propose a temperature-insensitive optical modulator based on a cascaded microring assistant MZI structure, where the radius of microrings coupled to each arm of the MZI increases linearly to obtain a wide working spectrum. Similar to that in Ref. [2], the effect of slow-light in the microring is utilized to obtain a compact footprint while the fabrication of this waveguide is much easier than that of the photonic crystal waveguide used in Ref. [4]. The symmetrical structure of the MZIs used in the proposed optical modulators leads to their temperature stability. The tolerated variation of ambient temperature can be as high as 134 °C while the footprint is only 340 μm^2. Furthermore, the influence of fabrication tolerance and carrier absorption in a practical device is also discussed.

2. Setup and operating principle

The proposed modulator is based on a cascaded microring assistant MZI (CMA-MZI) structure as shown in Fig. 1. There is a balanced MZI and two groups of microrings, the radii of the microrings on each arm, denoted as $R_{11} \sim R_{1m}$ and $R_{21} \sim R_{2m}$, increase linearly while the structure of the MZI is symmetrical. To make the footprint more compact, all of the microrings are settled inside the MZI. The length of the phase shifter is denoted as L, the length of Y-splitter is D, and the width of the CMA-MZI is W. So the area of the CMA-MZI can be expressed as $W \times (2D + L)$. The p- and n-doped areas are also shown in Fig. 1. The electrically driven signal could be applied to only one group of microrings ($R_{11} \sim R_{1m}$ or $R_{21} \sim R_{2m}$) or both of them. The working states of the CMA-MZI could be denoted as "state on" and "state off". In the state of "state on", there is no refractive index difference between two arms of CMA-MZI and the phase difference is 0 so that the output of modulator is maximum, while in the state of "state off", there is a specific refractive index difference between two arms of the CMA-MZI and the phase difference is π so that the output is minimum.

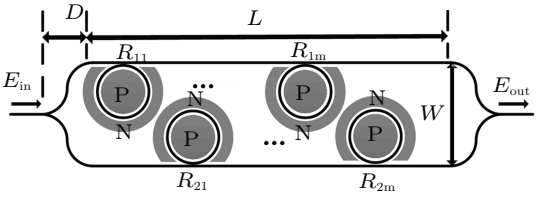


Fig. 1. Schematic plot of the cascaded microring assistant MZI modulator.

The optical transfer function of a balanced MZI is given by[6]

$$\begin{aligned} H &= \frac{E_{\rm out}}{E_{\rm in}} \\ &= \frac{1}{2}\left\{ \exp\left(-\frac{\alpha}{2}\right) [\exp(-{\rm j}\beta_1 L) \right. \\ &\quad \left. + \exp(-{\rm j}\beta_2 L)] \right\}, \end{aligned} \tag{1}$$

where α is the power attenuation constant, β is the propagation constant, and L is the length of phase shifter. So the output intensity is

$$\begin{aligned} I_{\rm out} &= |E_{\rm out}|^2 \\ &= I_{\rm in}\, {\rm e}^{-\alpha} \cos^2\left(\frac{\beta_1 L - \beta_2 L}{2}\right) \\ &= I_{\rm in}\, {\rm e}^{-\alpha} \cos^2\left(\frac{\Delta\varphi}{2}\right), \end{aligned} \tag{2}$$

where $I_{\rm in} = |E_{\rm in}|^2$ and $I_{\rm out}$ is determined only by the phase difference between the two arms. For a balanced MZI, when the ambient temperature changes, the phase variations of two arms are just the same so that the output of the MZI will not be influenced. It can be easily concluded that the excellent temperature stability of an MZI originates from the structure's symmetrical nature. However, the phase shifter of a conventional MZI modulator is usually long, owing to the weak plasma dispersion effect in Si. At a wavelength of 1.55 μm, the refractive index change Δn due to carrier injection can be expressed as[1]

$$\begin{aligned} \Delta n &= \Delta n_{\rm e} + \Delta n_{\rm h} \\ &= -[8.8 \times 10^{-22} \times \Delta n_{\rm e} \\ &\quad + 8.5 \times 10^{-18} \times (\Delta n_{\rm h})^{0.8}], \end{aligned} \tag{3}$$

where $\Delta n_{\rm e}$ and $\Delta n_{\rm h}$ are the changes in refractive index resulting from changes in the free-electron and free-hole carrier concentrations, respectively. From

Eq. (3), it can be found that the linear coefficients for $\Delta n_{\rm e}$ and $\Delta n_{\rm h}$ are very small so that the length of the MZI should be long enough or the drive voltage high enough to achieve a π phase shift. The phase responses of MZIs with different lengths are calculated (Fig. 2(a)), the parameters of waveguide are listed in Table 1. When the refractive index change between two arms of 0.002 is chosen, the length of phase shifter should be larger than 600 μm to obtain the π phase difference (Fig. 2(b)). In the state of "state-on", the phase delay of two arms is indicated with a solid curve; there is no phase difference between the two arms. In the state of state-off, the phase delay of one arm is represented with the dashed curve while the other arm is unchanged; so there is phase difference π between the two arms and the output power is minimum.

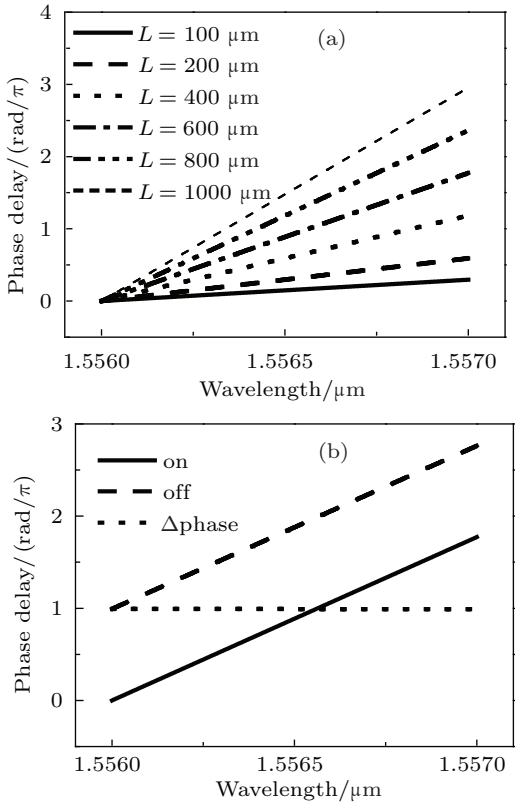


Fig. 2. Phase responses of a conventional MZI with different values of L (a), and in the case of L = 600 μm, when the refractive index changes 0.002 from "state on" to "state off", the phase changes π (b).

In order to reduce the footprint, the slow-light effect in the microring is utilized to increase the efficiency of the phase-shifter. So the length of the MZI can be shorter while the temperature stability remains good with the help of a balanced structure. For using the slow light effect in a microring, the phase response of the microring is more important than the amplitude response, so that the spectrum does not need to be very sharp and the fabrication tolerance can be improved. The optical transfer function of the microring is given by

$$H = \frac{E_{\rm out}}{E_{\rm in}} = \frac{t - \alpha\, {\rm e}^{-{\rm j}\beta L_{\rm ring}}}{1 - \alpha t\, {\rm e}^{-{\rm j}\beta L_{\rm ring}}}, \tag{4}$$

where $L_{\rm ring}$ is the circumference of the microring, t is the cross coupling coefficient of the microring to the bus waveguide. Via adjusting coupling coefficient t, the working state of a microring can be varied.[7] The amplitude responses and the phase responses in under, critical, and over-coupled states are shown in Fig. 3. It can be seen that there is a linear phase response range for each working state. But the widest wavelength range of linear phase response could be achieved at the over-coupled state (Fig. 3(b)). The curved slope can be manipulated by controlling t in an over-coupled state. Here, we change the parameter t by changing the spacing between the bus waveguide and the microring. When the variation of refractive index is given, a proper phase response can be obtained to realize π shift in a certain wavelength range ((Fig. 4(a))). Therefore, if two identical microrings over-coupled to

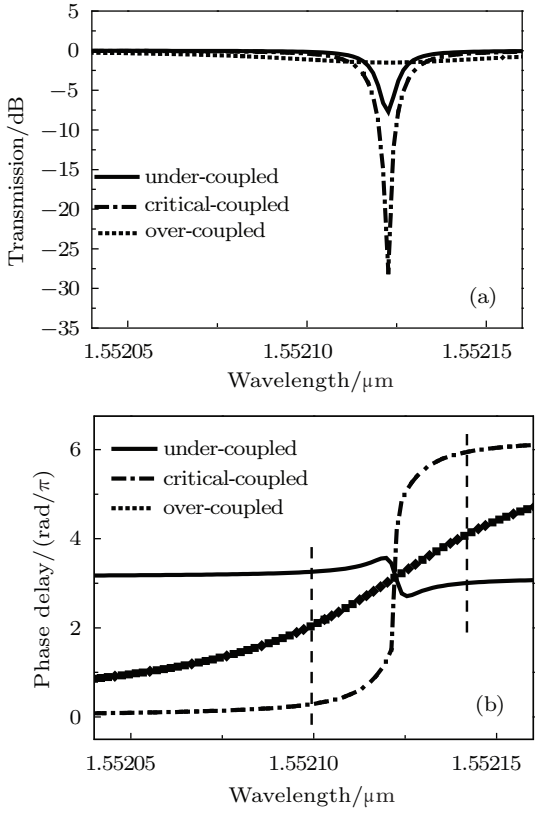


Fig. 3. Variations of transmission (a) and phase (b) with wavelength in three different coupling cases, with ring resonators each having a radius of 10 μm.

two arms of a balanced MZI, through varying the refractive index of one microring, the phase difference between two arms could be varied from 0 to π in a certain wavelength range. Furthermore, the extinction ratio in an over-coupled state is very poor (Fig. 3(a)) so the amplitude response of each arm of an MZI would not change much in the state of state-off.

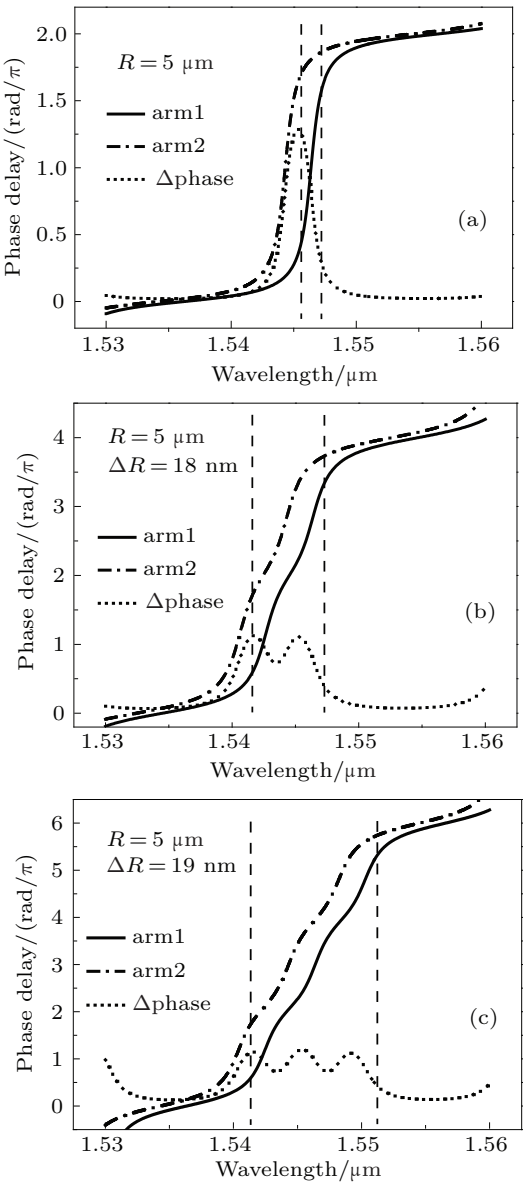


Fig. 4. Variations of phase delay with time of CMA-MZI modulator when the number of microrings on each arm is 1, 2, 3, respectively.

When more microrings are applied, the collective phase responses of all microrings will be superimposed together. The wavelength range of linear phase response can be extended when the resonant wavelength of each microring is staggered as shown in Fig. 4. The linear wavelength ranges are about 2 nm, 6 nm, and 10 nm in the cases from $m = 1$ to 3. To achieve this, the radius of microrings should be increased linearly in the proposed structure.

3. Simulation results and discussion

The numerical simulation is carried out with MATLAB. The equivalent FP model shown in Ref. [8] is used for microring calculation and the parameters are listed in Table. 1.

In Fig. 5(a), the simplest case of $m = 1$ is shown, where there is only one microring on each arm of MZI. The calculated transmission spectra of "on-state" and "off-state" are shown in Fig. 5(b). Firstly, the modulation depth of 7 dB and refractive index change of 0.005 are chosen. As shown in Fig. 5(b), the output power difference between the on-state and off-state is more than 7 dB at wavelength ranging from 1.5442 μm to 1.5465 μm. We define this wavelength range as operating wavelength range. The operating wavelength span is about 2.3 nm in the case of $m = 1$, which is optimized through scanning the spacing between the bus waveguide and the microring ($D_{\rm wm}$). When ambient temperature rises, the spectrum will be red-shifted as shown in Fig. 5(c). Due to operating in an over-coupled state, the spectrum of the CMA-MZI is not so narrow as that in a critical-coupled state so that the transmission ratio of on-state could be kept beyond a certain value. When the modulation wavelength is chosen to be 1.5465 μm at 0 °C, a temperature stability span of 30 °C can be obtained. We scan the ambient temperature from 0 °C to 35 °C, and the transmission spectra are shown in Fig. 5(c). Actually, the results in Figs. 5(b) and 5(c) only show the transmission spectra of state-on and state-off, when the refractive index changes gradually, the modulation curve is obtained as shown in Fig. 5(d). We can see that the 7-dB modulation depth can be maintained from 0 °C to 30 °C, but when the ambient temperature is beyond 30 °C, the modulation depth cannot reach 7 dB any more.

Table 1. Parameters used in calculation.

Width of the waveguide	500 nm	The refractive index of microring (without driven voltage)	3.45
Thickness of the waveguide	160 nm	The refractive index of microring (with driven voltage)	3.445
Waveguide loss	2 dB/cm	Thickness of the top silicon of SOI	220 nm

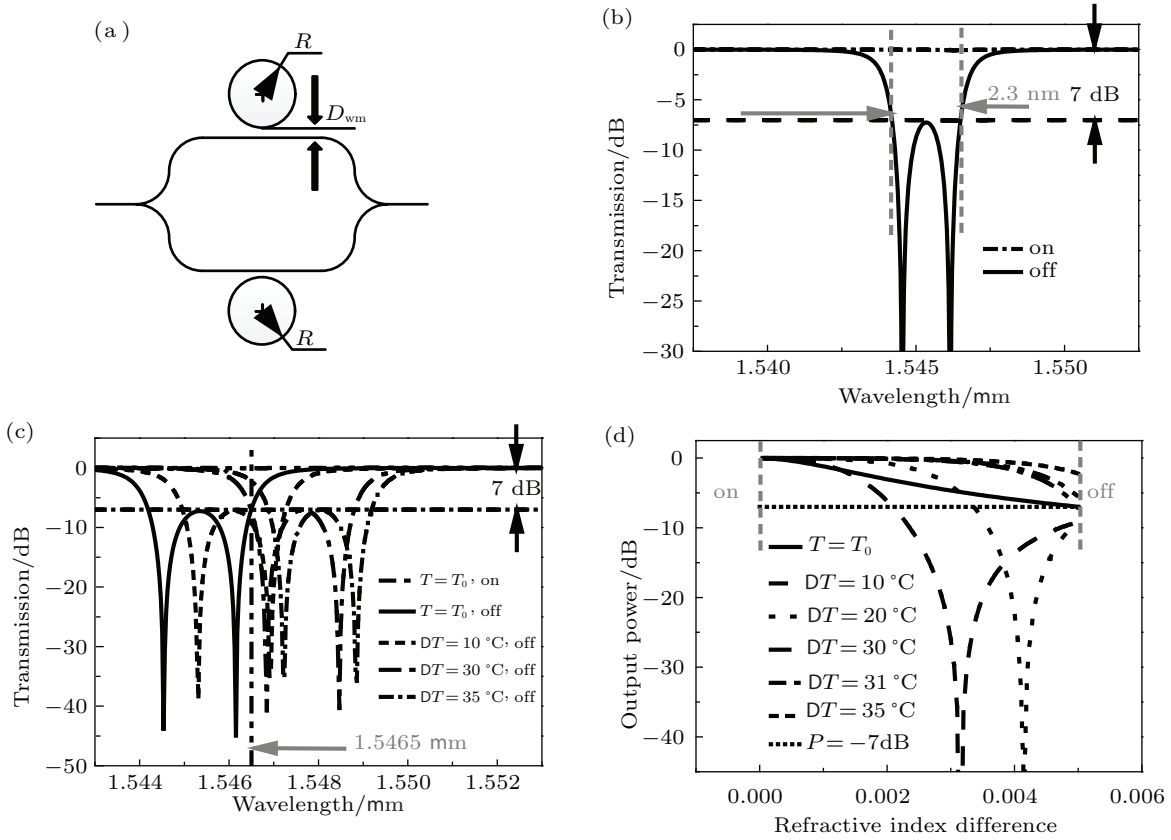


Fig. 5. Schematic plot (a), transmission spectra (b), (c), and modulation curves (d) of two-ring resonators over-coupled to a balanced MZI.

In order to obtain a wider temperature span, more microrings could be introduced. The radii of microrings in arms have a small difference (ΔR) so that the spectrum of every microring is staggered. Therefore, when an appropriate ΔR is settled, the available modulation wavelength span can reach a maximum value. In addition, the $D_{\rm wm}$ can also affect the result so both ΔR and $D_{\rm wm}$ are scanned in our calculation. Taking $m = 2$ for example (Fig. 6(a)), the optimal values of ΔR and $D_{\rm wm}$ ar 18 nm and 16 nm, respectively. The available wavelength span is 6.1 nm (Fig. 6(b)) and the corresponding temperature span is 76 °C. Similarly, if m is increased to 3 (Fig. 7(a)), the optimal values of ΔR and $D_{\rm wm}$ are 19 nm and 16 nm so that the available wavelength and temperature span are 10.3 nm (Fig. 7(b)) and 134 °C, respectively.

Actually, the modulation depth of 7 dB is overqualified while 5 dB is sufficient.[1] If modulation depth of 5 dB is chosen for calculation, the temperature stability is much better as the optical bandwidth is wider. The results of three aforementioned cases are 33 °C, 81 °C, and 142 °C, respectively.

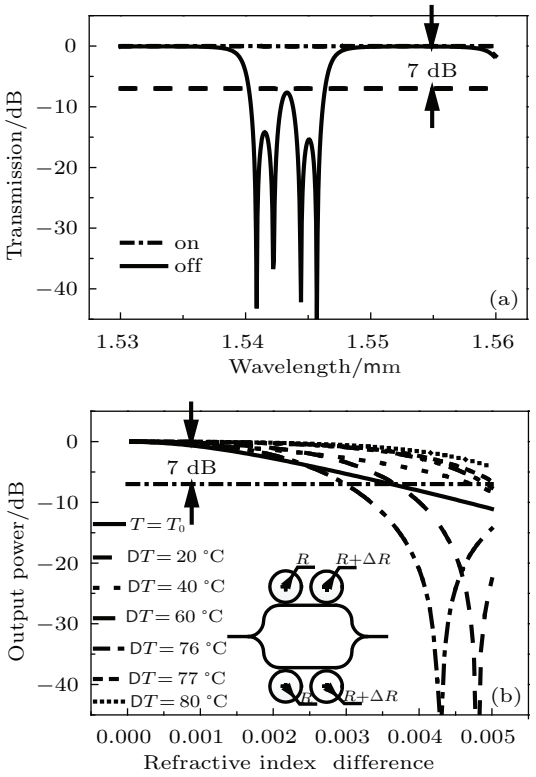


Fig. 6. Transmission spectra (a) and modulation curves (b) of four ring resonators over-coupled to a balanced MZI.

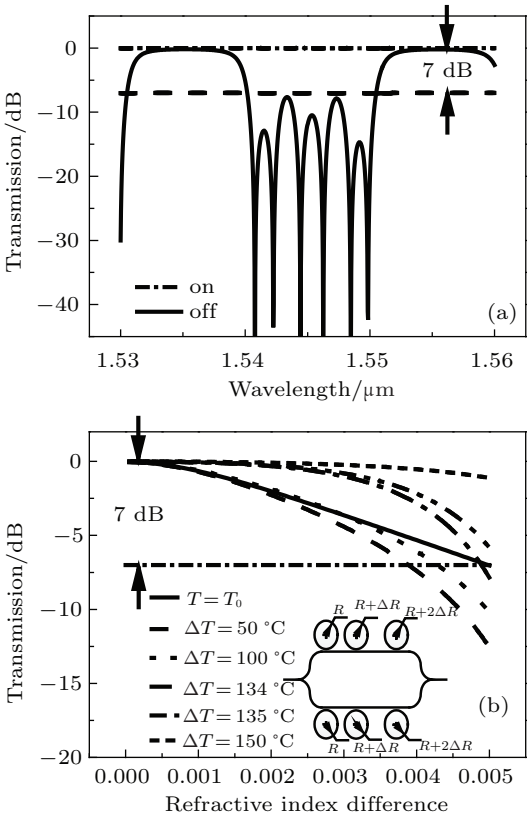


Fig. 7. Transmission spectra (a) and modulation curves (b) of six ring resonators over-coupled to a balanced MZI.

Until now, the temperature stability of our proposed CMA-MZI modulator has been discussed. For on-chip integration application, device footprint is another important issue. To make the proposed structure more compact, all of the microrings are placed inside the MZI as shown in Fig. 1 while the defined structural parameters are also shown. In order to show the compactness of our proposed modulator, we make a simple comparison among several types of structures. Since there is no report about the area of a practical MZI modulator, we first estimate the footprint of such modulator. Here the smallest reported W and D for MZI are chosen to be 4 μm and 2 μm, respectively[9] and the shortest length is taken to be 200 μm. Then the area of a practical MZI modulator is 800 μm^2 at least according to the state of arts. For our proposed modulator, W, D, and radius of microring is 10 μm, 2 μm, and 5 μm, respectively. Then for the case of $m = 1$, 2, 3 the estimated area of the whole modulator and the relevant tolerated temperature span are listed in Table 2. For the cases of $m = 1$–3, the footprints are 140 μm^2, 240 μm^2, and 340 μm^2, respectively. It could be seen that the footprint for each case is much smaller than that of MZI modulator, which is due to the help of the slow light effect of microrings. It should be mentioned that the footprint of electrode, which is not included in the aforementioned discussion, may be considered for a practical device. For a discrete device, the area for contact pad of ground-signal-ground (GSG) type is about 300 μm × 400 μm,[10] which is even much larger than that of Si MZI modulator, so that the footprint of a modulator is generally dominated by the electrode pads. At this point, the benefit of our proposed device is not so significant. However, for application of on-chip optical interconnection, the optical die could be linked to electrical layer through silicon vias (TSV) and three-dimensional (3D) integration technology.[11] According to International Technology Roadmap for Semiconductors (ITRS) 2010,[12] the diameter and pitch of TSV are 1 μm–2 μm and 2 μm–4 μm, respectively. And such values would be further reduced to 0.8 μm–1.5 μm and 1.6 μm–3 μm in 2015. Actually, such a small TSV can be easily fabricated in the device area shown in Fig. 1 with proper and careful design. In this work, we focus on the integrated Si modulator for optical interconnection on-chip rather than a discrete device so that the footprint of our proposed device is dominated by the waveguides and the microrings. That is also the reason why the area of the electrode pads is not included to evaluate the footprint of integrated silicon optical modulators.[1]

In our proposed structure, the coupling space $D_{\rm wm}$ is very critical as it determines the operating status of microring. For a practical device, the $D_{\rm wm}$ would be affected by the fabrication tolerance. In order to evaluate the influence of fabrication tolerance, we calculate the span of temperature stability, with varied $D_{\rm wm}$. Here, we assume that the device is fabricated by 180-nm standard CMOS process and the

Table 2. Estimated footprint and tolerated temperature span of an MZI modulator and a CMA-MZI with different parameters.

m	1	2	3	0
Footprint	$W*(2D+2R)$	$W*(2D+4R)$	$W*(2D+6R)$	$W*(2D+L)$
Footprint/μm^2	140	240	340	800
Temperature stability (°C) ER = 7 dB	30	76	134	–
Temperature stability (°C) ER = 5 dB	33	81	142	–

fabrication tolerance is 15% (∼30 nm). Then the $D_{\rm wm}$ is randomly set to be a value within 16±15 nm for the case of $m = 3$. By repeating the calculation 200 times, the static distribution of temperature span is shown in Fig. 8. It could be seen that temperature span of ∼60% of the calculated cases can maintain 130 °C while 6% of those is within 86 °C–94 °C and 34% of those is lower than 56 °C. So it could be concluded that the fabrication tolerance of ±15 nm would lead to the deteriorated performance. However, in our calculation the fabrication tolerance is about twice as large as the optimal coupling space $D_{\rm wm}$ (16 nm), the obtained yield is still as high as ∼60%. So we believe that our proposed structure is very promising for practical devices.

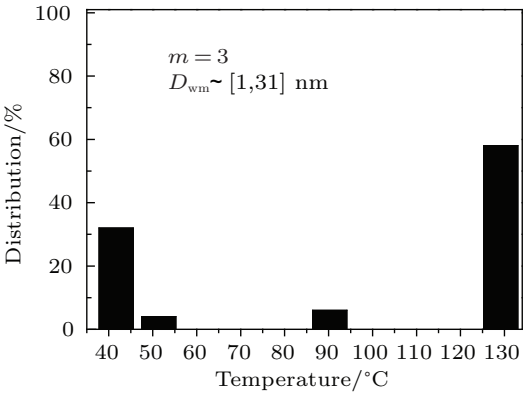


Fig. 8. Static distribution of temperature span with randomly varied coupling space $D_{\rm wm}$.

While designing a CMA-MZI, the $D_{\rm wm}$ is determined by the loss of microring, which could be introduced by the roughed sidewall of waveguide due to imperfect fabrication or by the carrier absorption due to Franz–Keldysh effect.[1] In our calculation, the waveguide loss is set to be 2 dB/cm and the carrier absorption is ignored. For a practical device, the $D_{\rm wm}$ should be carefully designed according to the waveguide loss and carrier absorption. As an example, we calculate the influence of carrier absorption for the case of $m = 3$. Here, the variation refractive index is assumed to be $\Delta n = \pm 0.0025$, then the density of carrier could be obtained from Eq. (3). Then the additional loss carrier absorption could be calculated from the folllowing relation:

$$\begin{aligned}\Delta\alpha &= \Delta\alpha_{\rm e} + \Delta\alpha_{\rm h} \\ &= 6.0\times10^{-18}\times\Delta n_{\rm e} + 4.0\times10^{-18}\times\Delta n_{\rm h}. \quad (5)\end{aligned}$$

The calculated value is about 0.16 dB. With the same parameter of $D_{\rm wm} = 16$ nm shown in Fig. 7(b), the temperature span of stable operation would be deteriorated to 120 °C (ER = 7 dB). For obtaining the same temperature span as that in Fig. 7(b), the $D_{\rm wm}$ should be optimized as 28 nm for considering the carrier absorption.

As discussed above, the influences of fabrication tolerance and carrier absorption should be considered for designing a practical device with optimal structure parameters. However, the operating principles of our proposed CMA-MZI would be still valid.

4. Conclusions

A compact and temperature-insensitive modulator with a microring assistant MZI structure on the silicon-on-insulator platform is proposed and demonstrated with numerical simulation. With the help of the slow light effect of over-coupled microrings, a higher-efficiency phase-shifter is obtained so that the footprint of MZI modulator is reduced. Due to the symmetrical nature of the MZI structure, high temperature stability is also obtained. The radius of microrings increases linearly to obtain linear phase response in a wider wavelength span. When the modulation depth is 7 dB, it is found that the stable temperature spans are 30 °C, 76 °C, and 134 °C for cases of $m = 1$, 2, and 3, respectively. At the same time, the corresponding footprints of our proposed CMA-MZI are estimated to be 140 μm^2, 240 μm^2, and 340 μm^2, respectively. The area of the most compact MZI is estimated to be 800 μm^2 with the reported optimal value. Finally, the influences of fabrication tolerance and carrier absorption in a practical device are also discussed. These results indicate that our proposed CMA-MZI modulator provides an approach to achieving a compact and temperature-insensitive optical modulator with CMOS compatible process.

Acknowledgement

The authors would like to thank Zhang Wei, Cui Kai-Yu, and Zhao Qiang for their valuable discussions and helpful comments.

References

[1] Reed G T, Mashanovich G, Gardes F Y and Thomson D J 2010 *Nature Photon.* **4** 661
[2] Green, W M J, Rooks M J, Sekaric L and Vlasov Y A 2007 *Opt. Express* **15** 17106
[3] Han M and Wang A 2007 *Opt. Lett.* **32** 1800

[4] Manipatruni S, Dokania R K, Schmidt B, Sherwood-Droz N, Poitras C B, Apsel A B and Lipson M 2008 *Opt. Lett.* **33** 2185

[5] Guha B, Kyotoku B B C and Lipson M 2010 *Opt. Express* **18** 3487

[6] Lawetz C, Cartledge J C, Rolland C and Yu J 1997 *J. Lightwave Technol.* **15** 697

[7] Sacher W D and Poon J K S 2009 *J. Lightwave Technol.* **27** 3800

[8] Zhang D, Feng X and Huang Y 2012 *Chin. Opt. Lett.* **10** 021302

[9] Vlasov Y A and McNab S J 2004 *Opt. Express* **12** 1622

[10] Li Z, Zhou L, Hu Y, Xiao X, Chu T, Yu Y and Yu J 2012 *Optoelectron.* **5** 90

[11] Lee B G, Biberman A, Chan J and Bergman K 2010 *IEEE Journal of Selected Topics in Quantum Electronics* **16** 6

[12] http://www.itrs.net/Links/2010ITRS/Home2010.htm [2010-]